

# Closed-loop Tracking Control of Poloidal Magnetic Flux Profile in Tokamaks

Y. Ou, C. Xu, E. Schuster, T. C. Luce, J. R. Ferron, M. L. Walker and D. A. Humphreys

**Abstract**—The potential operation of a tokamak fusion reactor in a highly-efficient, steady-state mode is directly related to the achievement of certain types of radial profiles for the current flowing toroidally in the reactor. The time evolution of the toroidal current profile is related to the poloidal magnetic flux profile evolution, which is modeled in cylindrical coordinates using a nonlinear partial differential equation (PDE) usually referred to as the magnetic diffusion equation. In this paper, we propose a framework to solve a closed-loop, finite-time, optimal tracking control problem for the poloidal magnetic flux profile via diffusivity, interior, and boundary actuation. The proposed approach is based on reduced order modeling via proper orthogonal decomposition (POD) and successive optimal control computation for a bilinear system. Simulation results illustrate the performance of the proposed controller.

## I. INTRODUCTION

A tokamak is a toroidal nuclear fusion reactor where magnetic fields are used to confine a high-temperature ( $\sim 10^8$  K) ionized gas or plasma (Fig. 1). At this temperature, the nuclei of two light atoms such as hydrogen have enough kinetic energy to overcome the Coulomb barrier (both nuclei carry positive charges), to fuse into a heavier nuclei, and to release energy  $E$  due to the amount  $\Delta m$  of matter “lost” in the process according to Einstein’s famous equation  $E = \Delta mc^2$  ( $c$  denotes the speed of light).

The magnetic field lines twist their way around the tokamak to form a helical structure. It is possible to use the poloidal component  $B_{pol}$  of the helicoidal magnetic lines to define nested toroidal surfaces corresponding to constant values of the poloidal magnetic flux. The poloidal flux  $\psi$  at a point  $P$  is the total flux through the surface  $S$  bounded by the toroidal ring passing through  $P$ , i.e.,  $\psi = \int B_{pol} dS$ . The dynamics of the poloidal flux  $\psi$  is governed in normalized cylindrical coordinates by a nonlinear parabolic partial differential equation (PDE) usually referred to as the magnetic diffusion equation, where the spatial coordinate corresponds to the minor radius of the torus. The magnetic diffusion equation allows three types of control mechanisms: interior control, boundary control, and diffusivity control. Each one of these control inputs is a combination of three physical actuators: the plasma total current, the non-inductive power, and the average plasma density.

This work was supported in part by a grant from the Commonwealth of Pennsylvania, Department of Community and Economic Development, through the Pennsylvania Infrastructure Technology Alliance (PITA), the NSF CAREER award program (ECCS-0645086), and DoE contract number DE-FC02-04ER54698. Y. Ou (yoo205@lehigh.edu), C. Xu and E. Schuster are with the Department of Mechanical Engineering and Mechanics, Lehigh University, Bethlehem, PA 18015, USA. T. C. Luce, J. R. Ferron, M. L. Walker and D. A. Humphreys are with the DIII-D tokamak, General Atomics, San Diego, California, USA.

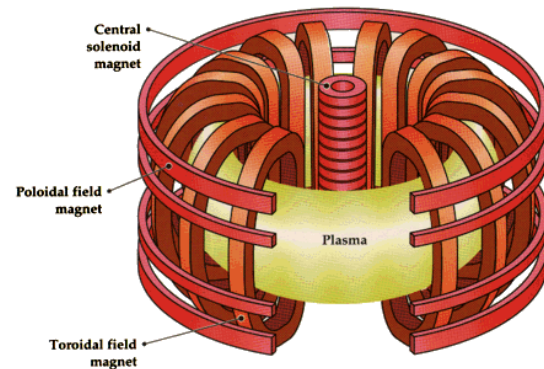


Fig. 1. Scheme of a tokamak device. The toroidal field (TF) coils are wrapped “poloidally” around the torus (the short way, going through the center hole), while the poloidal field (PF) coils are wrapped “toroidally” (the long way) around the torus. Current flowing in these conducting coils as well as in the plasma (inductively generated by the central solenoid) produces the helical magnetic field that confines the plasma. Source: PPPL.

Setting up a suitable current profile, which is proportional to the spatial derivative of the poloidal flux profile, has been demonstrated to be a key condition for one possible advanced scenario with improved confinement and possible steady-state operation [1]. One approach to current profile control is to focus on creating the desired current profile during the plasma current ramp-up and early flattop phases with the aim of maintaining this target profile during the subsequent phases of the discharge. Since the actuators that are used to achieve the desired target profile are constrained, experiments have shown that some of the desirable target profiles may not be achieved for all arbitrary initial conditions. In practice, the objective is to achieve the best possible approximate matching at time  $t_f = T$  during the early flattop phase of the total plasma current pulse, as shown in Fig. 2. Thus, such matching problem can be formulated as a finite-time optimal control problem for the magnetic diffusion PDE.

Our previous and current work includes the investigation of the use of extremum seeking [2] and nonlinear programming [3] to achieve an open-loop solution for this optimal control problem. The work is aimed at saving long trial-and-error periods of time currently spent by fusion experimentalists trying to manually adjust the time evolutions of the actuators to achieve the desired current profile at some prespecified time. However, the reproduction of the nominal initial conditions is usually challenging for the operators, who can only guarantee that the real initial conditions are within a neighborhood of the nominal ones. Therefore, in this work we propose a closed-loop optimal control law aimed at eliminating the effect of the disturbances in initial conditions by tracking the open-loop optimal control trajectory.

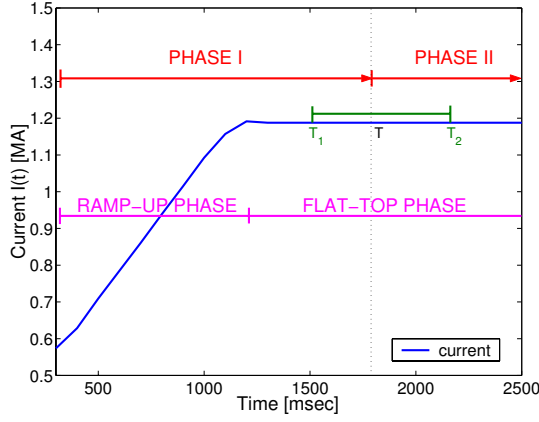


Fig. 2. Current Evolution.

Optimal feedback control design for nonlinear PDE systems is very challenging and usually unfeasible due to the high dimensionality of the problem. In this paper, we use proper orthogonal decomposition (POD) and Galerkin methods to obtain a low dimensional dynamical model for the nonlinear PDE system. The POD method is an efficient approach to extract the dominant dynamics from the infinite dimensional systems and to obtain low-dimensional ordinary differential equation (ODE) dynamical models from data ensembles arising from numerical simulation or experimental observation. The method has been widely and successfully used, particularly in the area of fluid dynamics (e.g., [4], [5], [6], [7]). Fundamental aspects of the POD method applied to parabolic problems, such as error estimates for the POD-Galerkin model reduction method applied to both linear and nonlinear systems, are discussed in [8].

Due to the presence of the diffusivity control term in the magnetic diffusion equation, the low dimensional dynamical model obtained turns to be bilinear. To track the open loop control trajectory for any initial condition, minimize the control effort, and match a target profile as closely as possible at a prespecified time  $t_f$ , a closed-loop finite-time optimal tracking control problem for a finite-dimensional bilinear system must be solved. The two-point boundary value (TPBV) problem arising from the optimality conditions for the bilinear system is solved using a convergent scheme based on the successive quasi-linear approximation approach proposed in [9], [10], [11].

This paper is organized as follows. In Section II, an infinite-dimensional dynamic model for the poloidal flux  $\psi$  is introduced. Section III describes the control objectives during the different phases of the tokamak discharge, and states the control problem. In Section IV, we discuss the POD method as well as the Galerkin projection method based on a test function set composed by dominant POD modes. After obtaining a low dimensional bilinear system, we derive the optimality conditions in Section V. In Section VI, we propose an iterative convergent scheme, based on the quasi-linear approximation method, to compute the optimal control. A simulation study showing the effectiveness of the proposed feedback controller is presented in Section VII. Conclusions and identified future work are presented in Section VIII.

TABLE I  
DESCRIPTION OF PARAMETERS

Parameters	Description
$\psi$	poloidal flux
$\rho_b$	effective radius of last closed flux surface
$\hat{\rho}$	normalized radius $\rho/\rho_b$
$\eta(T_e)$	plasma resistivity
$T_e$	electron temperature
$\tilde{J}_{NI}$	non-inductive source of current density
$\tilde{B}$	toroidal magnetic field
$\langle \cdot \rangle$	flux-surface average
$\mu_o = 4\pi \times 10^{-7} \text{ (H/m)}$	vacuum permeability
$B_{\phi,o} = 1.85 \text{ T}$	reference toroidal magnetic field at $R_o$
$R_o = 1.668 \text{ (m)}$	reference point for $B_{\phi,o}$ (e.g., geometric center of plasma $R_{geo}$ )
$\hat{F}, \hat{G}, \hat{H}$	Geometric factors (functions of $\hat{\rho}$ ) [12]
$I$	total plasma current
$P_{tot}$	total power applied
$\bar{n}$	spatially averaged density

## II. CURRENT PROFILE EVOLUTION MODEL

We let  $\rho$  be an arbitrary coordinate indexing the magnetic surface. Any quantity constant on each magnetic surface could be chosen as the variable  $\rho$ . We choose a geometric radius of the magnetic surface for the variable  $\rho$ , defined by  $\pi B_{\phi,o} \rho^2 = \Phi$ , where  $\Phi$  is the toroidal magnetic flux enclosed within the surface. The variable  $\hat{\rho}$  denotes the normalized radius  $\rho/\rho_b$ , and  $\rho_b$  is the effective radius of the last closed flux surface. The evolution of the poloidal flux in normalized cylindrical coordinates is given by the magnetic diffusion equation [12] (all the parameters are defined in Table I),

$$\frac{\partial \psi}{\partial t} = \frac{\eta(T_e)}{\mu_o \rho_b^2 \hat{F}^2 \hat{\rho}} \frac{\partial}{\partial \hat{\rho}} \left( \hat{\rho} \hat{F} \hat{G} \hat{H} \frac{\partial \psi}{\partial \hat{\rho}} \right) - R_o \hat{H} \eta(T_e) \frac{\langle \tilde{J}_{NI} \cdot \tilde{B} \rangle}{B_{\phi,o}}. \quad (1)$$

The boundary conditions of (1) are given by

$$\left. \frac{\partial \psi}{\partial \hat{\rho}} \right|_{\hat{\rho}=0} = 0, \quad \left. \frac{\partial \psi}{\partial \hat{\rho}} \right|_{\hat{\rho}=1} = \frac{\mu_o}{2\pi} \frac{R_o}{\hat{G}|_{\hat{\rho}=1} \hat{H}|_{\hat{\rho}=1}} I(t), \quad (2)$$

where  $I(t)$  denotes the total plasma current.

During ‘‘Phase I’’ (see Fig. 2), mainly governed by the ramp-up phase, the plasma current is mostly driven by induction. In this case, it is possible to decouple the equation for the evolution of the poloidal flux from the evolution equations for the temperature  $T_e(\hat{\rho}, t)$  and the density  $n_e(\hat{\rho}, t)$ . Highly simplified models for the temperature and non-inductive toroidal current density are chosen for this phase. The profiles are assumed to remain fixed. The responses to the actuators are simply scalar multiples of the reference profiles  $T_e^{profile}(\hat{\rho})$  and  $J_{NI}^{profile}(\hat{\rho})$ . These reference profiles are taken from a DIII-D tokamak discharge [12].

The resistivity  $\eta$  scales with the temperature  $T_e$  as  $\eta(\hat{\rho}, t) = k_{eff} Z_{eff} / T_e^{3/2}(\hat{\rho}, t)$ , where  $Z_{eff} = 1.5$ , and  $k_{eff} = 4.2702 \cdot 10^{-8} \text{ (}\Omega\text{m(keV)}^{3/2}\text{)}$ . The temperature is assumed to follow

$$T_e(\hat{\rho}, t) = k_{Te} T_e^{profile}(\hat{\rho}) \frac{I(t) \sqrt{P_{tot}}}{\bar{n}(t)}, \quad (3)$$

where  $k_{Te} = 1.7295 \cdot 10^{10} \text{ (m}^{-3}\text{A}^{-1}\text{W}^{-1/2}\text{)}$ ,  $P_{tot}$  is the total power of the non-inductive current sources (Electron Cyclotron Heating (ECH), Neutral Beam Heating (NBH), etc.), and  $\bar{n}(t)$  is the spatially averaged density.

The non-inductive toroidal current density is assumed to follow

$$\frac{\langle \bar{J}_{NI} \cdot \bar{B} \rangle}{B_{\phi,o}} = k_{NIpar} j_{NIpar}^{profile}(\hat{\rho}) \frac{I(t)^{1/2} P_{tot}(t)^{5/4}}{\bar{n}(t)^{3/2}}, \quad (4)$$

where  $k_{NIpar} = 1.2139 \cdot 10^{18} (m^{-9/2} A^{-1/2} W^{-5/4})$ .

We consider  $\bar{n}(t)$ ,  $I(t)$ , and  $P_{tot}(t)$  as the physical actuators of the system.

### III. CONTROL PROBLEM DESCRIPTION

The control objective, as well as the dynamic models for current profile evolution, depend on the phases of the discharge (Fig. 2). During ‘‘Phase I’’ the control goal is to drive the current profile from any arbitrary initial condition to a prescribed target or desirable profile at some time  $T \in (T_1, T_2)$  (here  $T_1 = 1.2s$  and  $T_2 = 2.4s$ ) in the flat-top phase of the total current  $I(t)$  evolution. However, since the available actuators during ‘‘Phase I’’ differ from those used during ‘‘Phase II,’’ and are constrained, the prescribed target profile is not an equilibrium profile during ‘‘Phase I’’. During ‘‘Phase II’’ the control goal is to regulate the current profile using as little control effort as possible because the actuators are not only limited in power but also in energy. For this reason, the goal during ‘‘Phase I,’’ and the focus of this work, is to set up an initial profile for ‘‘Phase II’’ as close as possible to its desired profile.

It is worth to note that we can rewrite the equation for the evolution of the poloidal flux (1) as

$$\frac{1}{f_1(\hat{\rho})} \frac{\partial \psi}{\partial t} = u_1(t) \frac{1}{\hat{\rho}} \frac{\partial}{\partial \hat{\rho}} \left( \hat{\rho} f_4(\hat{\rho}) \frac{\partial \psi}{\partial \hat{\rho}} \right) + f_2(\hat{\rho}) u_2(t) \frac{1}{f_1(\hat{\rho})} \quad (5)$$

with boundary conditions

$$\left. \frac{\partial \psi}{\partial \hat{\rho}} \right|_{\hat{\rho}=0} = 0, \quad \left. \frac{\partial \psi}{\partial \hat{\rho}} \right|_{\hat{\rho}=1} = k_3 u_3(t), \quad (6)$$

and where

$$f_1(\hat{\rho}) = \frac{k_{eff} Z_{eff}}{k_{Te}^{3/2} \mu_o \rho_b^2} \frac{1}{\hat{F}^2(\hat{\rho}) (T_e^{profile}(\hat{\rho}))^{3/2}} \quad (7)$$

$$f_2(\hat{\rho}) = - \frac{k_{eff} Z_{eff} R_o k_{NIpar}}{k_{Te}^{3/2}} \frac{\hat{H}(\hat{\rho}) j_{NIpar}^{profile}(\hat{\rho})}{(T_e^{profile}(\hat{\rho}))^{3/2}} \quad (8)$$

$$k_3 = \frac{\mu_o}{2\pi} \frac{R_o}{\hat{G}|_{\hat{\rho}=1} \hat{H}|_{\hat{\rho}=1}} = 1.0817 \cdot 10^{-7} \quad (9)$$

$$f_4(\hat{\rho}) = \hat{F} \hat{G} \hat{H}, \quad (10)$$

and  $u_1(t) = \left( \frac{\bar{n}(t)}{I(t) \sqrt{P_{tot}}} \right)^{3/2}$ ,  $u_2(t) = \frac{\sqrt{P_{tot}(t)}}{I(t)}$ ,  $u_3(t) = I(t)$ .

It is important to note that the magnetic diffusion equation (5) admits control not only through  $u_2(t)$  (interior control) and  $u_3(t)$  (boundary control) but also through  $u_1(t)$ , what we name *diffusivity control* in this paper. Although interior (see, e.g., [13] and references therein) and boundary control [14] of parabolic diffusion-reaction PDE equations such as (5) have been extensively studied, diffusivity control has been rarely considered.

## IV. MODEL REDUCTION USING POD/GALERKIN

### A. POD Modes

The set  $\mathcal{V} = \text{span}\{y_1, \dots, y_n\} \subset \mathbb{R}^m$  refers to a data ensemble consisting of the snapshots  $\{y_j\}_{j=1}^n$  obtained from the simulation of the system (1) on the grid  $\mathcal{Q}_{ij} = (x_i, t_j)$ , where  $i, j$  are integers with  $1 \leq i \leq m$ ;  $1 \leq j \leq n$  ( $y_j(i) = \psi(x_i, t_j)$ ). Let  $\{\phi_k\}_{k=1}^d$  be the orthonormal basis of the data ensemble  $\mathcal{V}$ , where  $d = \dim \mathcal{V} \leq m$ . The goal of the POD method is to find a subset of  $l$  eigenfunctions of the basis  $\{\phi_k\}_{k=1}^d$  such that for some predefined  $1 \leq l \leq d$  the following average index is minimized

$$\min_{\{\phi_k\}_{k=1}^l} \frac{1}{n} \sum_{j=1}^n \left\| y_j - \sum_{k=1}^l (y_j, \phi_k) \phi_k \right\|^2, \quad (11)$$

subject to  $(\phi_i, \phi_j) = \delta_{ij}, 1 \leq i \leq l, 1 \leq j \leq l,$

where  $(\cdot, \cdot)$  denotes the inner product and  $\|y\| = \sqrt{y^T y}$ . The solution of (11) can be found in the literature, e.g., [4], [8].

### B. Galerkin Projection

Let  $V = \{z|z, \frac{dz}{dx} \in L^2(\hat{\rho})\}$ , and  $\phi(\hat{\rho}) \in V$  be a test function, where  $\hat{\rho} \in [0, 1]$ . By multiplying both sides of (5) by  $\hat{\rho} \phi(\hat{\rho})$ , integrating by parts over the spatial domain  $[0, 1]$ , and taking into account the boundary conditions, we obtain the *weak form* ( $F' = \frac{\partial F}{\partial \hat{\rho}}$ )

$$\begin{aligned} & \frac{\partial}{\partial t} \int_0^1 \hat{\rho} \frac{1}{f_1(\hat{\rho})} \phi(\hat{\rho}) \psi(\hat{\rho}, t) d\hat{\rho} \\ & = u_1(t) u_3(t) \phi(1) f_4(1) k_3 \\ & + u_2(t) \int_0^1 \hat{\rho} \phi(\hat{\rho}) f_2(\hat{\rho}) \frac{1}{f_1(\hat{\rho})} d\hat{\rho} \\ & - u_1(t) \int_0^1 f_4(\hat{\rho}) \phi'(\hat{\rho}) \psi'(\hat{\rho}, t) \hat{\rho} d\hat{\rho}, \end{aligned} \quad (12)$$

Let  $V_{POD} = \text{span}\{\phi_1, \phi_2, \phi_3, \phi_4, \dots, \phi_l\} \subset V$  be a space consisting of the POD modes from the model reduction process, and substitute  $\psi(\hat{\rho}, t) \approx \psi^l(\hat{\rho}, t) = \sum_{k=1}^l \alpha_k(t) \phi_k(\hat{\rho})$  in (12), where  $\phi_k(\hat{\rho}) \in V_{POD}$ ,  $k = 1, 2, \dots, l$ . Using the notation

$$\begin{aligned} M_{jk} &= \langle \phi_k, \phi_j \frac{1}{f_1} \rangle = \int_0^1 \phi_k(\hat{\rho}) \phi_j(\hat{\rho}) \frac{1}{f_1(\hat{\rho})} \hat{\rho} d\hat{\rho} \\ K_{jk} &= \langle f_4 \phi_k', \phi_j' \rangle = \int_0^1 f_4(\hat{\rho}) \phi_k'(\hat{\rho}) \phi_j'(\hat{\rho}) \hat{\rho} d\hat{\rho} \\ P_j &= \langle \phi_j, \frac{f_2}{f_1} \rangle = \int_0^1 \phi_j(\hat{\rho}) f_2(\hat{\rho}) \frac{1}{f_1(\hat{\rho})} \hat{\rho} d\hat{\rho} \\ Q_j &= f_4(1) k_3 \phi_j(1), \end{aligned} \quad (13)$$

and redefining the control vector as  $u = (v_1, v_2, v_3)^T = (u_1, u_2, u_1 u_3)^T$ , we obtain a matrix representation for the reduced order model

$$M \frac{dx}{dt} = -K x v_1(t) + P v_2(t) + Q v_3(t), \quad (14)$$

where  $x(t) = (\alpha_1, \dots, \alpha_l)^T \in \mathbb{R}^l$ ,  $M, K \in \mathbb{R}^{l \times l}$ ,  $P, Q \in \mathbb{R}^l$  and  $v_i(t) \in \mathbb{R}^1$  ( $i = 1, 2, 3$ ). The vector  $x(t)$  is the finite dimensional approximation, with respect to the obtained POD modes, of  $\psi(\hat{\rho}, t)$ . The components of the initial state are given by  $x^i(t_0) = x_0^i = (\psi(t_0), \phi_i)$ ,  $i = 1, \dots, l$ , where  $x_0 \in \mathbb{R}^{l \times 1}$  and  $\phi_i$ , for  $i = 1, \dots, l$ , are the POD modes.

## V. OPTIMAL TRACKING CONTROL DESIGN

By inverting the matrix  $M$ , we can write the equation (14) as follows

$$\frac{dx}{dt} = -M^{-1}Kxv_1(t) + M^{-1}Pv_2(t) + M^{-1}Qv_3(t). \quad (15)$$

We let  $v^o(t) = [v_1^o \ v_2^o \ v_3^o]^T$  be a set of open-loop control trajectories, which are computed off-line, and  $x^o(t)$  be the open-loop state trajectory associated to the open-loop control  $v^o(t)$ , with a nominal initial state  $x_0^o$ . The open-loop state trajectory satisfies

$$\frac{dx^o}{dt} = -M^{-1}Kx^ov_1^o(t) + M^{-1}Pv_2^o(t) + M^{-1}Qv_3^o(t), \quad (16)$$

with initial condition  $x^o(t_0) = x_0^o$ .

Let us define  $e(t) = x(t) - x^o(t)$ ,  $v^c(t) = v(t) - v^o(t)$ , where  $v(t) = [v_1 \ v_2 \ v_3]^T$  is the total control inputs and  $v^c(t) = [v_1^c \ v_2^c \ v_3^c]^T$  is the to-be-designed closed-loop control, which is appended to the open-loop control  $v^o(t)$ . Then, we can write

$$\frac{de}{dt} = A(t)e + B(e)u(t) \quad (17)$$

where,  $A(t) = -M^{-1}Kv_1^o(t) \in \mathbb{R}^{l \times l}$ ,  $B(e) = [-M^{-1}K(e + x^o) \ M^{-1}P \ M^{-1}Q] \in \mathbb{R}^{l \times 3}$ ,  $u(t) = v^c(t) = [v_1^c \ v_2^c \ v_3^c]^T \in \mathbb{R}^{3 \times 1}$ .

We state the optimal control problem for the reduced order ODE system (17) as

$$\min_u J = \frac{1}{2}e^T(t_f)Se(t_f) + \frac{1}{2} \int_{t_0}^{t_f} e^T(t)\Omega(t)e(t)dt + u^T(t)R(t)u(t)dt, \quad (18)$$

where  $S$  and  $\Omega$  are symmetric positive semi-definite matrices and  $R$  is a symmetric positive definite matrix.

By introducing the lagrange multiplier  $\lambda(t) \in \mathbb{R}^{l \times 1}$ , we can define the Hamiltonian

$$H(e, u, \lambda) = \frac{1}{2}e^T(t)\Omega(t)e(t) + \frac{1}{2}u^T(t)R(t)u(t) + \lambda^T(t)[A(t)e(t) + B(e)u(t)]. \quad (19)$$

By invoking the principle of optimality,  $\frac{\partial H}{\partial u} = 0$ , we obtain the optimal control

$$u^*(t) = -R^{-1}(t)B^T(e)\lambda(t). \quad (20)$$

The optimal solution is characterized by the following sets of differential equations for the state  $e$  and costate  $\lambda$  (two-point-boundary-value problem)

$$\dot{e} = \frac{\partial H}{\partial \lambda} = A(t)e + B(e)u(t) \quad (21)$$

$$\dot{\lambda} = -\frac{\partial H}{\partial e} = -\Omega(t)e - A(t)^T\lambda(t) - u^T(t)\frac{\partial B^T(e)}{\partial e}\lambda(t). \quad (22)$$

The boundary conditions are

$$e(t_0) = e_0 = x_0 - x_0^o, \quad \lambda(t_f) = Se(t_f). \quad (23)$$

## VI. QUASI-LINEAR APPROXIMATION

The solution of the nonlinear TPBV problem is usually computationally demanding. In this section, we propose a successive approach based on the Quasi-linear approximation [9], [10], [11] to solve the two-point boundary value problem on-line. By expanding our problem (17) up to first-order around the previous iteration trajectories  $e^k(t)$  and  $u^k(t)$ , the system takes the form

$$\dot{e}^{k+1} = A(t)e^{k+1} + B^k(t)u^{k+1}(t), \quad (24)$$

where  $k$  is the iteration number and

$$B^k(t) = B(e)|_{e^k(t)}, \quad (25)$$

with initial condition  $e^{k+1}(0) = e_0$ . The new cost function

$$J^{k+1} = \frac{1}{2}(e^{k+1})^T Se^{k+1} + \frac{1}{2} \int_{t_0}^{t_f} (e^{k+1})^T(t)\Omega(t)e^{k+1}(t) + (u^{k+1})^T(t)R(t)u^{k+1}(t)dt. \quad (26)$$

For each iteration, we have now a standard linear quadratic optimal control problem defined by (24) and (26) with the approximate optimal control law given by

$$u^{k+1}(t) = -R^{-1}(t)(B^k)^T(t)\lambda^{k+1}(t). \quad (27)$$

At each iteration, the two-point boundary value problem (21)-(22) reduces to

$$\begin{aligned} \dot{e}^{k+1} &= A(t)e^{k+1} + B^k(t)(-R^{-1}(t)(B^k)^T(t)\lambda^{k+1}(t)) \\ \dot{\lambda}^{k+1} &= -\Omega(t)e^{k+1}(t) - A(t)^T\lambda^{k+1}(t), \end{aligned} \quad (28)$$

along with the boundary condition

$$e^{k+1}(t_0) = e_0, \quad \lambda^{k+1}(t_f) = Se^{k+1}(t_f). \quad (29)$$

Let us propose the solution form,

$$\lambda^{k+1}(t) \triangleq s^{k+1}(t)e^{k+1}(t), \quad (30)$$

where  $s^{k+1}(t)$  is a  $l \times l$  symmetric matrix. Substituting (30) into the equation of (28), we can obtain the following Riccati matrix differential equation

$$\dot{s}^{k+1} = -A^T s^{k+1} - s^{k+1}A - \Omega + s^{k+1}B^k R^{-1}(B^k)^T s^{k+1}, \quad (31)$$

with terminal condition

$$s^{k+1}(t_f) = S.$$

Then, the closed-loop system becomes

$$\dot{e}^{k+1} = (A - B^k R^{-1}(B^k)^T s^{k+1})e^{k+1}, \quad (32)$$

with the initial condition  $e^{k+1}(t_0) = e_0$ .

The open-loop state trajectories  $x^o(t)$  are used to evaluate (25) and start the iterations. The iterative procedure is stopped when convergence is achieved under given error tolerance. Finally, by using the convergent solution of the Riccati equations (31), we obtain the following feedback control law

$$u^*(t) = -R^{-1}(t)B^T(e)s(t)e(t). \quad (33)$$

To satisfy the magnitude constraints of the actuators, we can always increase the values of the elements of the weight matrix  $R$ .

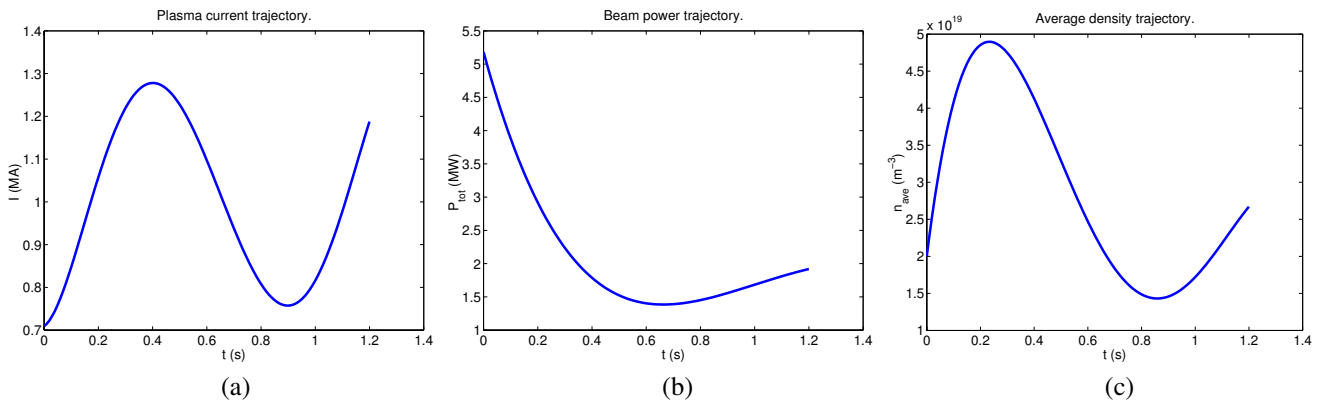


Fig. 3. Open-loop extremum seeking (ES) optimal control inputs: (a)  $I(t)$ , (b)  $P_{tot}$ , (c)  $\bar{n}(t)$ .

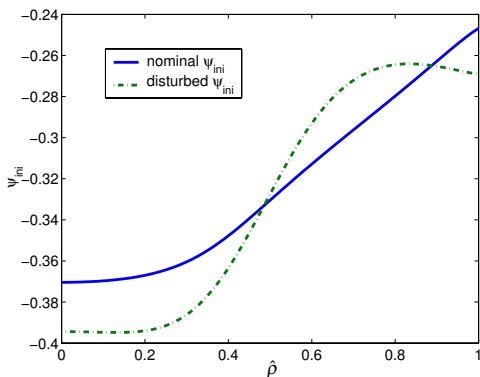


Fig. 4. Comparison of initial  $\psi$  profiles.

## VII. SIMULATION STUDY

In this section, we present simulation results showing the effectiveness of the proposed optimal control algorithm in a disturbance rejection problem. For this simulation study we consider the time interval  $[t_0 = 0, t_f = T = 1.2s]$ .

The nominal initial poloidal flux  $\psi_{ini}$  shown in Fig. 4 has been considered for the synthesis of an open-loop optimal controller via Extremum Seeking [2]. The time evolution of the open-loop control inputs  $v^o(t)$  obtained from the off-line Extremum Seeking optimization procedure are shown in Fig. 3. Fig. 5-(a) illustrates the space-time evolution of the poloidal flux  $\psi(t, \hat{\rho})$  as determined by the original PDE system (1) for the nominal initial poloidal flux  $\psi_{ini}$  and the Extremum-Seeking-based open-loop control inputs  $v^o(t)$ .

By simulating the original PDE system (1), a data ensemble is created with snapshots of  $\psi(t, \hat{\rho})$ . We then extract POD modes from the created data ensemble. The four most dominant POD modes are shown in Fig. 5-(b). With these four POD modes, we construct a low dimensional dynamical system governed by the ordinary differential equation (ODE) system (15). Before computing the closed loop control based on the reduced-order model, we assess the effectiveness of the reduced-order model in approximating the original PDE system. Fig. 5-(c) shows the approximation error as function of time and space. The order of the error demonstrate that the reduced-order model based on only four POD modes can successfully approximate the PDE system.

For the cost functional (18), we choose  $\Omega(t) \equiv \Omega = \mathbb{I}^{l \times l}$  ( $\mathbb{I}$  is an identity matrix,  $l = 4$ ),  $S(t) \equiv S = \text{diag} \{20, 5, 0.1, 0.1\}$ , and  $R(t) \equiv R = \text{diag} \left\{ \frac{1}{\max(v_1^o)}, \frac{50}{\max(v_2^o)}, \frac{1}{\max(v_3^o)} \right\}$ , where  $\max(v_i^o)$  stands for the maximum value of the open-loop control  $v_i^o(t)$ . We use the proposed quasi-linear approximation scheme to compute the optimal control. After the first iteration  $k = 1$ , the solution of the Riccati matrix equation converges, and the feedback controller is implemented according to (33).

We consider now a disturbed initial profile  $\psi_{ini}$ , as shown in Fig. 4, and compare the performances of both open-loop and closed-loop controllers in the presence of this disturbance. In the case of the open-loop controller, the control input trajectories shown in Fig. 3, and computed for the nominal initial profile, are used. In the case of the closed-loop controller, the control input trajectories are shown in Fig. 6. Fig. 7 shows the differences between the final-time profiles  $\psi(t_f, \hat{\rho})$  obtained with the open-loop and closed-loop controllers and the desired target profile  $\psi^d$ . Both final-time profiles are obtained using the disturbed initial profile. It is possible to note from Fig. 7 that the closed-loop controller can reduce the matching error caused by the disturbance in the initial flux profile. It is also possible to note that the matching by the closed-loop controller is not perfect. However, this does not imply a limitation of the closed-loop controller but a consequence of the imposed constraints for the actuators (the matrix  $R$  was selected to keep the actuator trajectories within physical ranges).

## VIII. CONCLUSIONS AND FUTURE WORKS

In this paper, we consider a simplified dynamic model describing the evolution of the poloidal flux during the inductive phase of the tokamak discharge. Using this PDE model, and the POD/Garlekin technique, we derive a low dimensional dynamical system which preserves the dominant dynamics of the original parabolic PDE system. We propose a convergent successive scheme based on the quasi-linear approximation to compute an optimal tracking control for the reduced order system. The simulation study shows that the proposed controller overcome to some extent the disturbances in the initial poloidal flux profile.

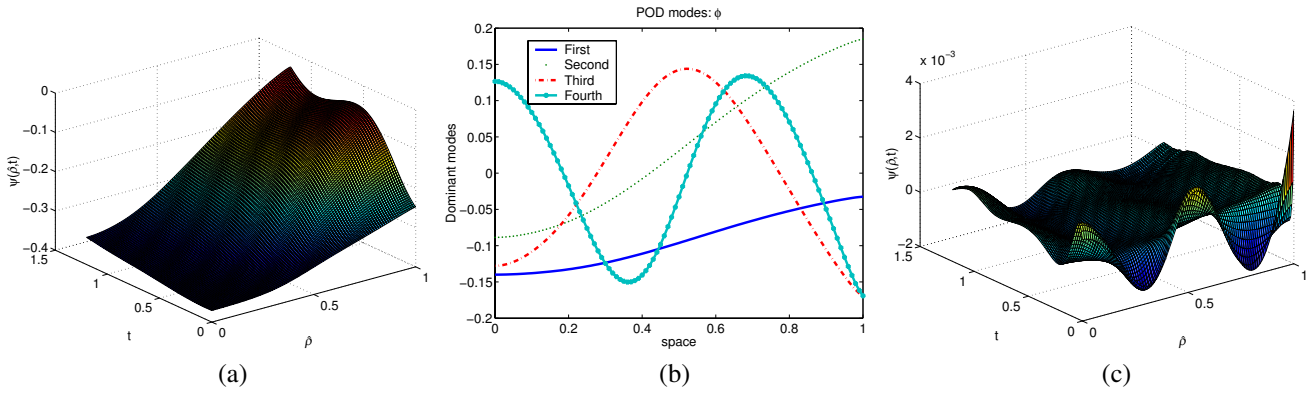


Fig. 5. (a) Evolution of  $\psi$  generated from the original PDE model, (b) Four more energetic POD modes (the corresponding SVD eigenvalues are  $\Lambda_1 = 5597.403$ ,  $\Lambda_2 = 161.413$ ,  $\Lambda_3 = 1.643$ ,  $\Lambda_4 = 0.0522$ ), (c) The evolution of  $\psi$  reconstructed from the reduced ODE model.

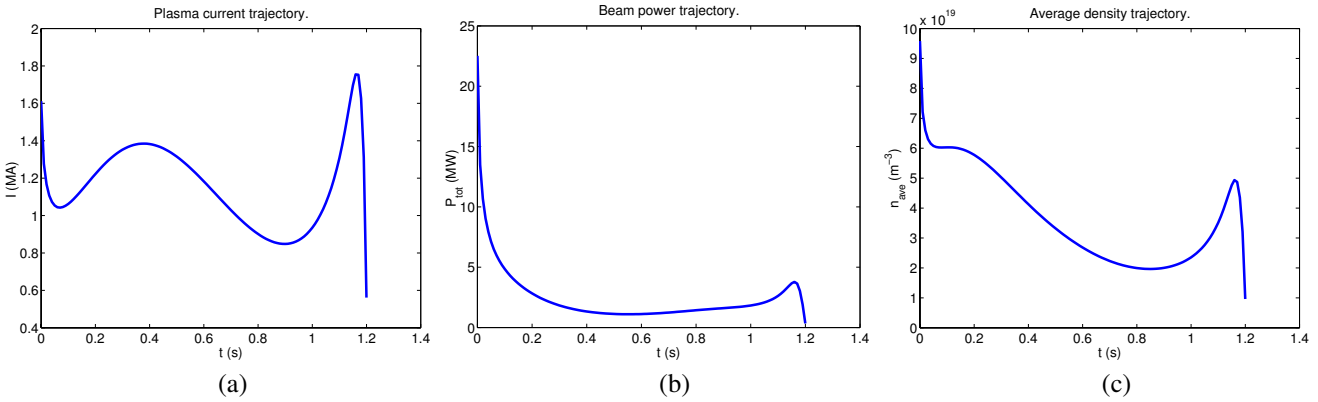


Fig. 6. Optimal tracking control: (a)  $I(t)$ , (b)  $P_{tot}$ , (c)  $\bar{n}(t)$ .

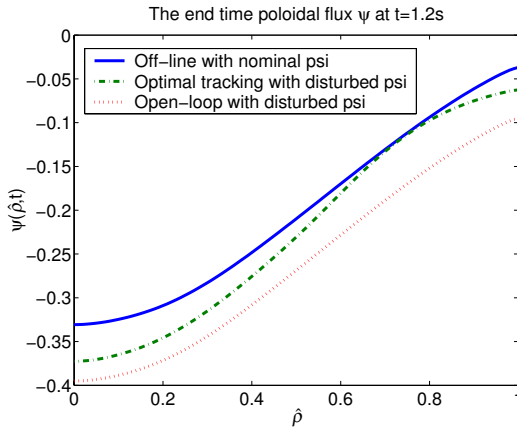


Fig. 7. Final time  $\psi$  matching comparison.

From the point of view of this fusion application, future work includes reformulating the optimal control problem in order to set as the primary goal not the matching of a desired target profile for the poloidal flux but the matching of a desired target profile for its spatial derivative. In addition to magnitude constraints, it is also necessary to consider constraints in the rate and in the initial/final values of the actuators. Finally, the experimental validation of this controller at the DIII-D tokamak is also part of our future work.

#### REFERENCES

- [1] M. Murakami *et al.*, "Progress toward fully noninductive, high beta conditions in DIII-D," *Physics of Plasmas*, vol. 13, no. 5, p. 056106, 2006.
- [2] Y. Ou *et al.*, "Extremum-seeking finite-time optimal control of plasma current profile at the DIII-D tokamak," in *Proceedings of the 26th American Control Conference*, 2007.
- [3] C. Xu *et al.*, "POD-Based Optimal Control of the Current Profile in Tokamak Plasmas via Nonlinear Programming," in *Proceedings of the 27th American Control Conference*, 2008.
- [4] P. Holmes, J. Lumley, and G. Berkooz, *Turbulence, coherent structures, dynamical systems and symmetry*. New York: Cambridge University Press, 1996.
- [5] K. Kunisch and S. Volkwein, "Control of the Burgers equation by a reduced-order approach using proper orthogonal decomposition," *Journal of Optimization Theory and Applications*, vol. 102, pp. 345–371, 1999.
- [6] M. Hinze and K. Kunisch, "Three control method for time-dependent fluid flow," *Flow, Turbul. and Combustion*, vol. 65, pp. 273–298, 2000.
- [7] M. Bergmann, L. Cordier, and J. Brancher, "Optimal rotary control of the cylinder wake using proper orthogonal decomposition reduced-order model," *Physics of Fluids*, vol. 17, pp. 097 101 (1–21), 2005.
- [8] K. Kunisch and S. Volkwein, "Galerkin proper orthogonal decomposition methods for parabolic problems," *Numerische Mathematik*, vol. 90, pp. 117–148, 2001.
- [9] Z. Aganovic and Z. Gajic, "The successive approximation procedure for finite-time optimal control of bilinear systems," *IEEE Transactions on Automatic Control*, vol. 39, pp. 1932–1935, 1994.
- [10] X. Xu and S. K. Agrawal, "Finite-time optimal control of polynomial systems using successive suboptimal approximations," *Journal of Optimization Theory and Applications*, vol. 105, pp. 477–489, 2000.
- [11] G. Tang, "Suboptimal control for nonlinear systems: a successive approximation approach," *Systems & Control Letters*, vol. 54, pp. 429–434, 2005.
- [12] Y. Ou, E. Schuster, T. Luce, J. Ferron, M. Walker, and D. Humphreys, "Towards model-based current profile control at DIII-D," *Fusion Engineering and Design*, vol. 82, pp. 1153–1160, 2006.
- [13] P. Christofides, *Nonlinear and Robust Control of PDE Systems*. Birkhauser, 2001.
- [14] A. Smyshlyaev and M. Krstic, *Boundary Control of PDEs: A Short Course on Backstepping Designs*. SIAM, to appear.